Structure and Deformation of an Elastomeric Propylene–Ethylene Copolymer

B. C. Poon,[1*] P. Dias,[1] P. Ansems,[2] S. P. Chum,[2] A. Hiltner,[1] E. Baer[1]

[1]*Department of Macromolecular Science and Engineering, Center for Applied Polymer Research, Case Western Reserve University, Cleveland, Ohio 44106-7202*
[2]*Polyolefins and Elastomers R&D, The Dow Chemical Company, Freeport, Texas 77541*

Received 10 November 2005; accepted 31 May 2006
DOI 10.1002/app.25243
Published online in Wiley InterScience (www.interscience.wiley.com).

ABSTRACT: The elastic behavior of a propylene–ethylene copolymer was investigated. An initial ''conditioning'' tensile extension up to 800% strain resulted in an elastomer with low initial modulus, strong strain hardening, and complete recovery over many cycles. Structural changes that occurred in the low crystallinity propylene–ethylene copolymer during conditioning, and that subsequently imparted elastomeric properties to the conditioned material, were investigated. Thermal analysis, wide and small angle X-ray diffraction, and atomic force microscopy measurements were performed at various strains during the conditioning process. Conditioning transformed crystalline lamellae into shish-kebab fibers by melting and recrystallization. The fibers, accounting for only 5% of the bulk, were interconnected by a matrix of entangled, amorphous chains that constituted the remaining 95%. It was proposed that the shish-kebab fibers acted as a scaffold to anchor the amorphous rubbery network. Entanglements of the amorphous chain segments acted as network junctions and provided the elastic response. The stress–strain response of materials conditioned to 400% strain or more was described by the classical rubber theory with strain hardening. The extracted value of M_c, the molecular weight between network junctions, was intermediate between the entanglement molecular weights of polypropylene and polyethylene. J Appl Polym Sci 104: 489–499, 2007

Key words: elastomers; propylene–ethylene copolymers; shish-kebab fibers

INTRODUCTION

Thermoplastic elastomers are a class of materials that process like thermoplastics but exhibit the physical properties of vulcanized rubbers. Unlike vulcanized rubbers, where elasticity is derived from an amorphous network interconnected by chemical crosslinks, thermoplastic elastomers possess physical crosslinks. Commercially significant thermoplastic elastomers such as segmented polyurethanes and various styrene-based elastomers possess a blocky chain structure consisting of higher and lower glass-transition (T_g) segments. Phase separation of the higher T_g blocks creates the physical junctions that give these thermoplastic elastomers their rubbery behavior.[1]

Several reports describe olefinic copolymers that exhibit characteristics of thermoplastic elastomers. Low crystallinity, low density (0.86–0.88 g cm^{-3}) random ethylene–octene copolymers (EO) are elastomeric.[2] Unlike blocky thermoplastic elastomers, where phase separation creates the physical crosslinks, crystallizable ethylene sequences in EO elastomers form fringed micellar crystals that act as network junctions.[3] It is proposed that crystallizable chain segments at the edges of fringed micellar crystals undergo reversible detachment and reattachment upon stretching.[4] Accordingly, the stress–strain response of EO elastomers is satisfactorily described by a modification of the classical rubber theory that considers the fringed micellar crystals as mobile junctions or ''slip links.''

Recently, some experimental propylene-based elastomers have been synthesized by The Dow Chemical Company. These elastomers are low crystallinity propylene–ethylene (P/E) copolymers with $\sim$ 10–15 wt % ethylene that exhibit elastomeric properties with uniform deformation and high recovery from large strains. In contrast to the fringed micellar crystals of elastomeric EO, elastomeric P/E forms lamellar crystals. It follows that a structural model for deformation based on fringed micellar crystals is not appropriate for elastomeric P/E. A proposed model considers transformation of the lamellar crystals into shish-kebab fibers.[5–7] The small concentration of shish-kebab fibers acts as a scaffold for an elastomeric matrix of entangled, amorphous chains. The major features of the model are supported by recently published observations on a similar P/E copolymer.[8] The goal of the present work is to further examine the process whereby stretching transforms lamellar crystals into shish-kebab fibers and to probe the origin of the

**Present address:* The Dow Chemical Company, Freeport, Texas 77541
Correspondence to: A. Hiltner (pah6@cwru.edu).

elastomeric behavior. Comparisons are made with elastomeric EO.

EXPERIMENTAL

The P/E copolymer elastomer used in this study was supplied by The Dow Chemical Company. The copolymer (P/E) contained 19.4 mol % ethylene and had a weight average molecular weight of 2.6×10^5 g mol^{-1}. The density was 0.8618 g cm^{-3} and crystallinity was 5 wt % from the DSC heat of melting using a heat of fusion of 165 J g^{-1} for the polypropylene crystal.[9]

Films 0.5 mm thick were compression molded from the pellets. The pellets were sandwiched between Mylar® sheets and heated at 190°C for 10 min under minimal pressure, for 10 min at 10 MPa, and cooled to ambient temperature at $\sim$ 15°C min^{-1} in the press. Because aging associated with slow crystallization was especially noticeable in copolymers with higher ethylene content, experiments were performed on compression molded film after it was aged 7–12 days at ambient temperature.

Microtensile specimens were cut from the plaques according to ASTM D-1708. The specimens were cyclically loaded and unloaded in uniaxial tension at ambient temperature in an Instron 1123 at a crosshead speed of 22.3 mm min^{-1} (100% min^{-1} based on the initial microtensile geometry). The initial cycle is labeled the ''conditioning cycle.'' The specimen was subsequently unloaded and reloaded to the same crosshead displacement with the same crosshead speed. This is referred to as the ''first cycle.'' Unless indicated otherwise, 24 h elapsed between the conditioning cycle and the first cycle.

After conditioning to different strains, specimens weighing 5–10 mg were cut for thermal analysis. Thermograms were obtained from -50 to 190°C with a heating rate of 10°C min^{-1}. Thermal analysis was performed on a PerkinElmer Model 7 DSC.

Wide angle X-ray scattering (WAXS) patterns of specimens held at various conditioning strains were obtained using a Statton camera. The WAXS patterns were recorded on an image plate with an exposure time of 4 h and read with a Fujifilm FDL5000 image plate reader.

Small-angle X-ray scattering (SAXS) experiments were performed on stretched specimens at DND-CAT, Advanced Photon Source (APS), Argonne National Laboratory. The wavelength used was 0.82,656 Å. A MAR-CCD (MARUSA) two-dimensional detector was used for data collection with a sample-to-detector distance of 4144 mm and an exposure time of 200 s. The collected SAXS images were calibrated with the scattering pattern of silver behenate standard.

Atomic force microscopy (AFM) was performed on specimens held in the stretched state at various conditioning strains. Specimens for AFM were stretched at 30°C to conform to the slightly elevated temperature in the AFM. Specimens were imaged in a Digital Instruments Nanoscope IIIa using a special specimen holder to maintain the stretched state. Before imaging, the specimens were acid etched for 3 min using a 2 : 1 (vol:vol) solution of sulfuric acid:orthophosphoric acid with 0.7 wt % potassium permanganate.[10]

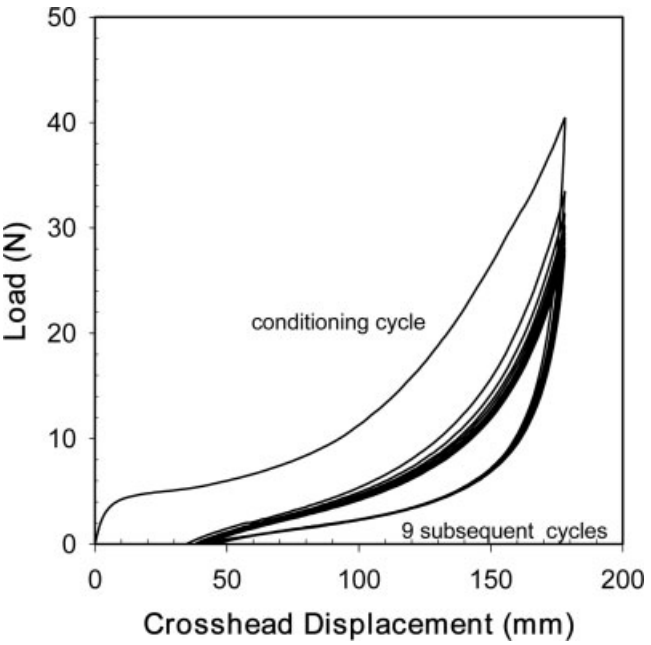

Figure 1 The conditioning loading and unloading cycle of P/E and the nine subsequent cycles for a conditioning strain of 800%.

RESULTS AND DISCUSSION

Conditioning process

The effect of repeated cyclic loading on the elastomeric behavior of P/E is shown in Figure 1. In this example, the specimen was cycled 10 times to 800% strain based on the initial gauge length with no time lapse between cycles. The initial loading and unloading cycle is designated as the ''conditioning cycle,'' and the subsequent cycle is the ''first cycle.'' There was considerable change in the stress response between the conditioning cycle and the first cycle. However, there was virtually no change among all subsequent cycles. The specimen exhibited some amount of permanent set after the conditioning cycle; however, it recovered completely on the first cycle and all subsequent cycles. Apparently, a permanent structural change occurred during the conditioning cycle that created a material with better elastomeric properties. Moreover, only one cycle was required to bring about the structural change. The conditioning process was standardized to a single loading and

unloading cycle at a rate of 100% min^{-1} at 21°C. The conditioned specimen was allowed to relax at ambient conditions for 24 h before further testing.

Conditioning curves for various strains are shown Figure 2(a). The conditioning stress–strain curve exhibited a distinct knee at low strain, followed by a plateau of gradually increasing stress that extended to about 400% strain, which marked the beginning of a strain-hardening region at higher strain. The permanent set, defined as $[(\ell - \ell_0)/\ell_0] \times 100$, where ℓ_0 is the initial gauge length and ℓ is the gauge length after the conditioning cycle, increased from 2 and 10% for conditioning strains of 100 and 200%, to 35, 80, and 115% for conditioning strains of 400, 600, and 800%, respectively. The conditioned specimens were subsequently loaded to the same crosshead displacement to obtain the first cycle. The first cycle stress–strain curves are plotted in Figure 2(b,c) to reflect the new gauge length and cross-sectional area after the conditioning cycle. The first cycle of specimens conditioned to 100 and 200% strain closely resembled the conditioning cycle, in particular a relatively sharp knee at low strain was followed by a plateau of gradually increasing stress [Fig. 2(b)]. Apparently, the conditioning strain was too low to impart much permanent structural change. Conditioning to 400% strain, close to the end of the plateau region, resulted in a less pronounced knee on the first cycle. Conditioning to 600 and 800% strain took the specimens into the strain-hardening region. Conditioning above 400% produced an increasingly large stress response on the first cycle [Fig. 2(c)]. The stress response of the specimen conditioned to 800% strain was five times higher than that of the specimen conditioned to 400%. The conditioned specimens showed essentially complete recovery. The cyclic loading behavior of specimens conditioned to higher strains resembled the behavior of a chemically crosslinked rubber with low initial modulus, uniform deformation to high strains, and complete recovery.

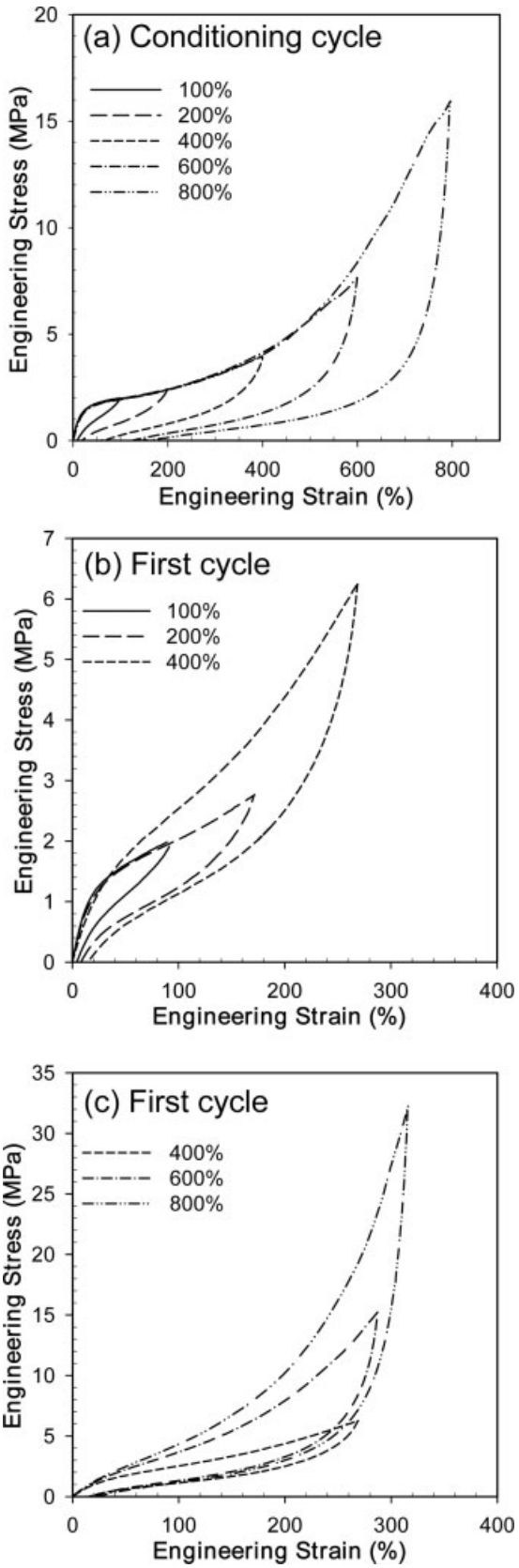

Figure 2 Effect of conditioning strain for P/E: (a) Conditioning cycles for different strains; (b) first cycle for conditioning strains of 100, 200, and 400%; and (c) first cycle for conditioning strains of 400, 600, and 800%.

Formation of elastic structure during conditioning

The structural origin of the enhanced elasticity of conditioned P/E was probed. The effect of conditioning strain on melting behavior is shown in Figure 3. The unconditioned polymer exhibited a small amount of crystallinity with a melting peak at 42°C. Because P/E crystallized very slowly, the melting endotherm was the result of aging at ambient temperature. Conditioning to 50% strain did not affect the melting behavior. After conditioning to 100% strain, a small melting endotherm appeared at 33°C. The lower melting endotherm gradually increased as the material was conditioned at progressively higher strains until it became the larger melting peak at 400% conditioning strain; and was the only melting endotherm in thermograms of materials conditioned to 600 and 800% strain. The

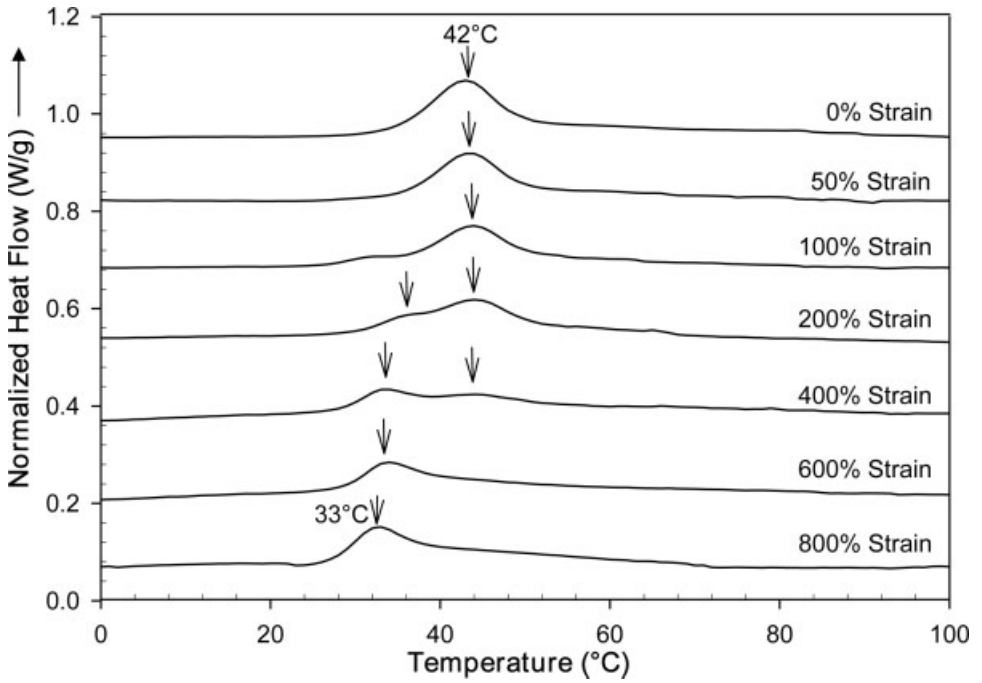

Figure 3 Effect of conditioning strain on the melting behavior of P/E.

thermograms suggested that the copolymer underwent gradual melting and recrystallization during conditioning. However, as indicated by the total melting enthalpy of 8–9 J g^{-1}, the amount of crystallinity remained essentially constant at about 5%.

Because of the low crystallinity of P/E, only two rings appeared in the WAXS pattern of the unconditioned material [Fig. 4(a)]. The inner ring corresponded to the 110 reflection of the polypropylene α-phase crystal. The more intense outer ring included the overlapping 040 reflection of the α-phase and the 008 reflection of the γ-phase.[11] The WAXS patterns of specimens held at various conditioning strains are also shown in Figure 4. Upon conditioning to 100% strain, the WAXS pattern remained essentially unchanged, although broad meridional concentration of the 110 intensity suggested some orientation of the lamellar axis into the stretch direction [Fig. 4(b)]. At 200% strain, the 110 and 040 rings transformed into equatorial spots, which suggested orientation of the chains into the stretch direction (*c*-axis orientation) [Fig. 4(c)]. Additional broad, weak 110 meridional arcs indicated some *a*′-axis orientation. The *a*′-axis orientation probably arose from epitaxial crystallization.[12,13]

The dual crystal orientation has been observed in polypropylene oriented near the melting point and in melt spun polypropylene fibers.[12,14,15] A faint ring overlaying the 040 spots indicated some amount of remaining γ-phase. Additional reflections of the polypropylene α-phase that were not strong enough to detect in the unstrained material appeared at 200% strain. They were the 130 equatorial spots and the 111,131 diagonal spots from crystals with *c*-axis orientation.

Increasing the conditioning strain from 200 to 400% resulted in sharpening of the α-phase reflections and disappearance of the γ-phase ring [Fig. 4(d)]. At 800% strain, the α-phase spots became sharper [Fig. 4(d)]. The 110 meridonial arcs resolved into spots with intensity maxima at azimuthal angles of $\pm 20^{\circ}$. The WAXS pattern at 800% strain resembled a well-oriented polypropylene fiber pattern with predominantly *c*-axis orientation and some *a*′-axis orientation.[16]

Corresponding SAXS measurements were made on the unconditioned material and on specimens conditioned to 200 and 800% strain. Absence of a SAXS ring from the unconditioned sample indicated that the lamellae were not well-organized into larger morphological structures [Fig. 5(a)]. At 200% conditioning strain, the SAXS pattern showed diffuse meridional arcs with a spacing of 14 nm [Fig. 5(b)], which transformed into intense lobes at 800% strain [Fig. 5(c)]. The meridional reflections stemmed from stacked lamellae preferentially oriented perpendicular to the stretching direction. The stacked lamellae had a long period of 20 nm. Depending on draw temperature and draw ratio, reported long spacings for polypropylene ranged from 13 to 26 nm.[17,18] The equatorial streaks suggested fibers oriented parallel to the stretch direction.[17,19] The structure of conditioned P/E inferred from WAXS and SAXS consisted of stacked lamellae arranged in fibers that were oriented parallel to the stretch direction. The stacked lamellae had predominantly *c*-axis orientation with some *a*′-axis orientation due to epitaxial crystallization.

Atomic force microscopy was used to directly image the structures inferred from WAXS and SAXS (Fig. 6).

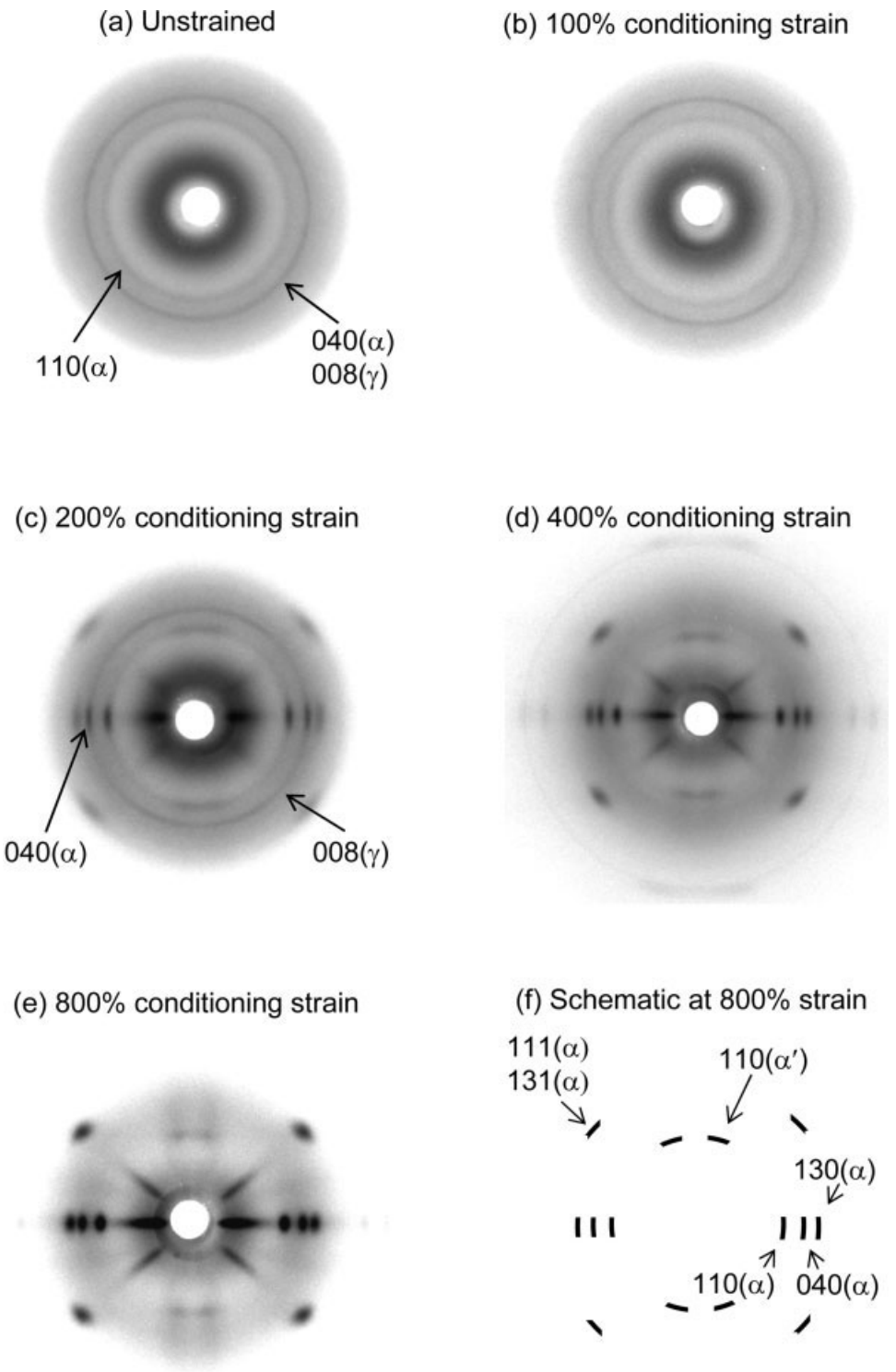

Figure 4 Effect of conditioning strain on the WAXD pattern of P/E: (a) Unstrained; (b) at 100% conditioning strain; (c) at 200% conditioning strain; (d) at 400% conditioning strain; (e) at 800% conditioning strain; and (f) schematic of the WAXD pattern at 800% strain. The stretching direction is vertical.

The images were captured in the stretched state after acid etching removed the amorphous material. In the unconditioned specimen, the crystalline morphology consisted mostly of individual randomly dispersed lamellae 12–15 nm thick [Fig. 6(a)]. Occasionally, a few lamellae were organized into embryonic axialites. Upon conditioning to 100% strain, the lamellae aligned somewhat into the stretching direction and started to break up into short lamellar segments [Fig. 6(b)]. At 200% conditioning strain, some of the broken lamellae appeared to

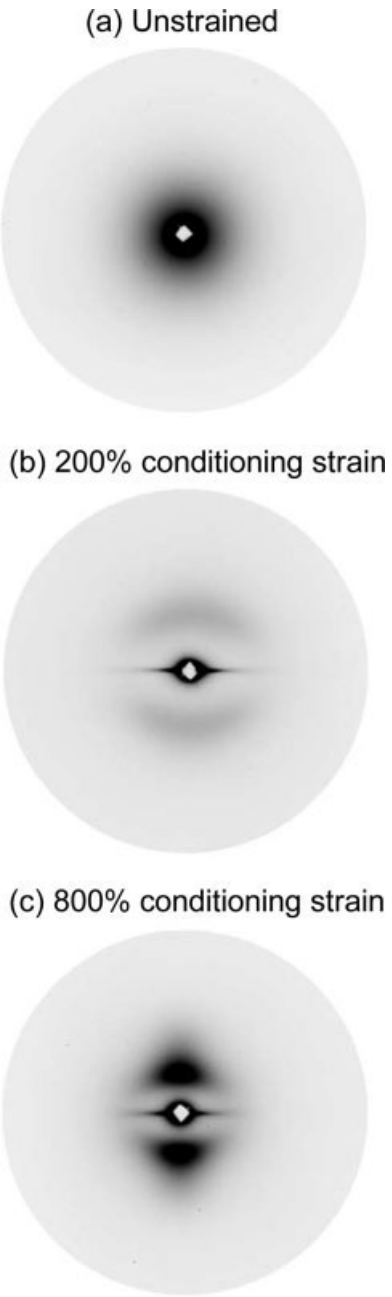

Figure 5 Effect of conditioning strain on the SAXD pattern of P/E: (a) Unstrained; (b) at 200% conditioning strain; and (c) at 800% conditioning strain.

reorganize into stacks (arrow) with the lamellar axis perpendicular to the direction of strain [Fig. 6(c)]. At 400% strain, numerous stacks of very short lamellae imparted an overall fibrous texture that resembled shish-kebabs fibers [Fig. 6(d)]. At 800% conditioning strain, the crystalline morphology was predominantly composed of long shish-kebab fibers [Fig. 6(e)]. In AFM images, the short lamellae were about 20 nm thick with a spacing of 20–30 nm between lamellae.

The WAXS pattern of P/E that was conditioned to 800% strain and unloaded retained the fiber pattern; however, broadening of the spots into arcs indicated some loss of fiber orientation [Fig. 7(a,b)]. Broadening of the lobes in the SAXS pattern also indicated loss in orientation of the stacked lamellae [Fig. 7(c,d)]. The long spacing decreased from 20 to 15 nm. The corresponding AFM image showed that the shish-kebab fibers remained after the load was removed; however, they underwent some loss of orientation [Fig. 8(a,b)].

A description of the structural changes that occur during conditioning of P/E is based on the combined results of AFM, WAXS, SAXS, and DSC. At lower conditioning strains (0–200% strain), randomly arranged lamellae orient to some extent into the stretching direction and breakup into small lamellar segments. The first indication of organized lamellar stacks in AFM images occurs at 200% strain. A corresponding level of orientation is seen in WAXS and SAXS patterns. The stacks become more numerous as the strain increases to 400%. The appearance of a second melting endotherm in DSC thermograms indicates that the transformation from dispersed lamellar to lamellar stacks is accompanied by melting and recrystallization. As the conditioning strain increases above 400%, the material experiences higher stresses as it is taken into the strain hardening region of the stress–strain curve. The stacks of short lamellae are transformed into shish-kebab fibers that give a highly oriented fiber pattern in the WAXS. Highly oriented, extended chains constitute the shish, short lamellar overgrowths form the kebabs.[20] The processes by which conditioning transforms randomly dispersed lamellar crystals of P/E into shish-kebab fibers are in accordance with the structural changes generally associated with yielding and drawing of lamellar crystals. However, because P/E has only 5% crystallinity, the shish-kebab fibers make up only a small fraction of the total structure. The fibers are embedded in a matrix of entangled amorphous chains that interconnect to the kebabs.

The proposed structural model for elastomeric behavior of conditioned P/E is shown schematically in Figure 9. The fibers, accounting for only 5% of the bulk, are interconnected by a matrix of entangled, amorphous chains that constitute the remaining 95%. The shish-kebab fibers act as a permanent scaffold that anchors the amorphous rubbery network. Entanglements of the amorphous chains act as network junctions and provide the elastic response. Constraints imposed by the shish-kebab fibers impart a strong stress response at higher strains. During recovery, retraction of the rubbery network causes the fibers to randomize to some extent. During reversible restretching, extension of the amorphous chains realigns the fibers in the stretch direction. Chain disentanglement during stretching is inhibited by anchoring of the amorphous chains in the lamellae of the shish-kebab fibers. As a consequence, the elastic behavior of conditioned P/E is retained over many stretching cycles.

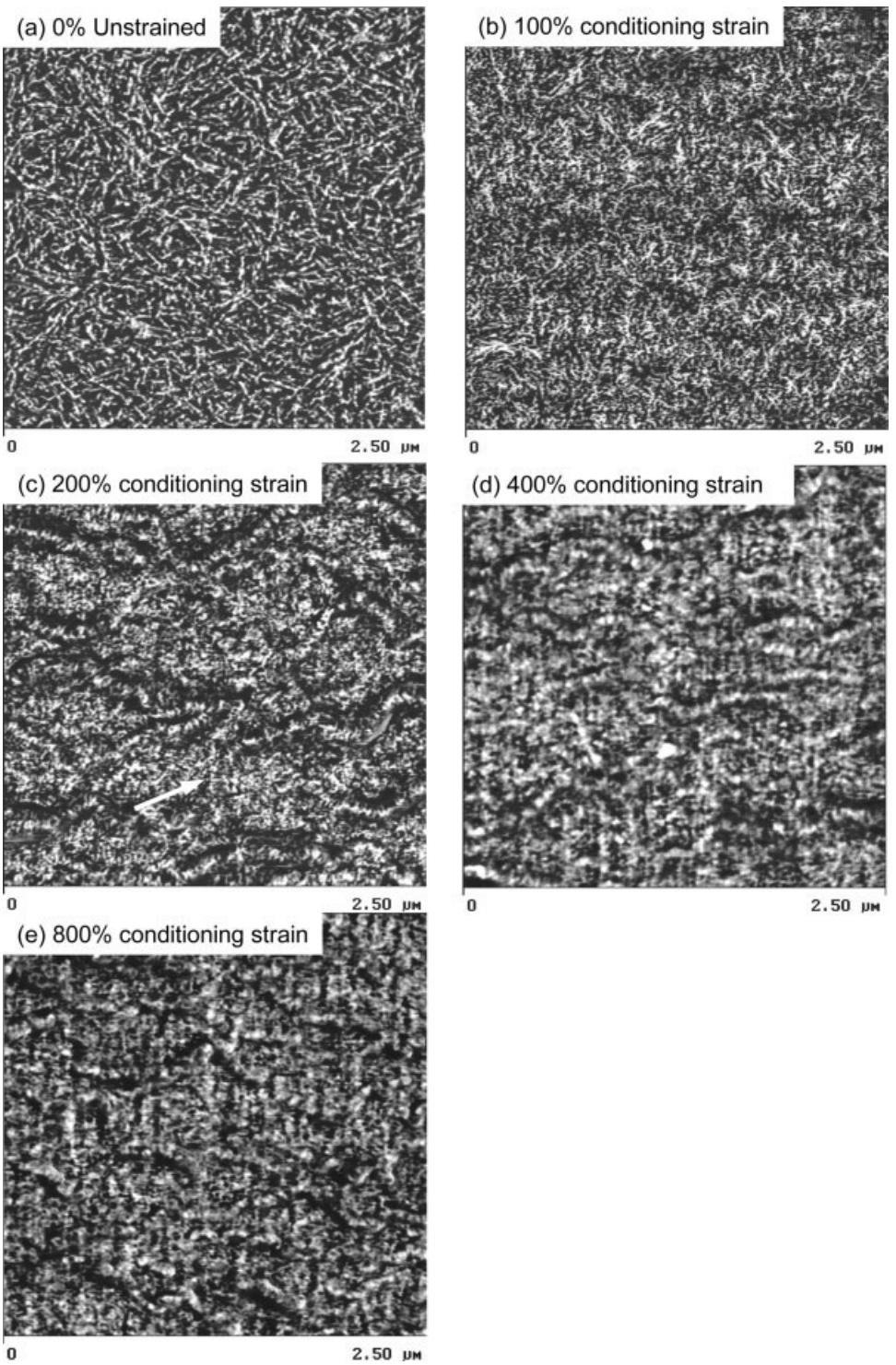

Figure 6 AFM phase images of P/E at various conditioning strains: (a) Unstrained; (b) at 100% conditioning strain; (c) at 200% conditioning strain; (d) at 400% conditioning strain; and (e) at 800% conditioning strain. The stretching direction is vertical. The wavy, horizontal features are an artifact.

Elastomeric behavior of conditioned structure

The loading stress–strain behavior was tested against the classical rubber theory modified for chain inextensibility. The expression for the equilibrium tensile response is[21,22]

$$\sigma = N_c kT\left(\lambda - \frac{1}{\lambda^2}\right)\left(\frac{1-\alpha^2}{(1-\alpha^2\varphi)^2} - \frac{\alpha^2}{1-\alpha^2\varphi}\right) \quad (1)$$

where σ is the stress, λ is the draw ratio, k is the Boltzmann constant, T is the temperature, N_c is density of

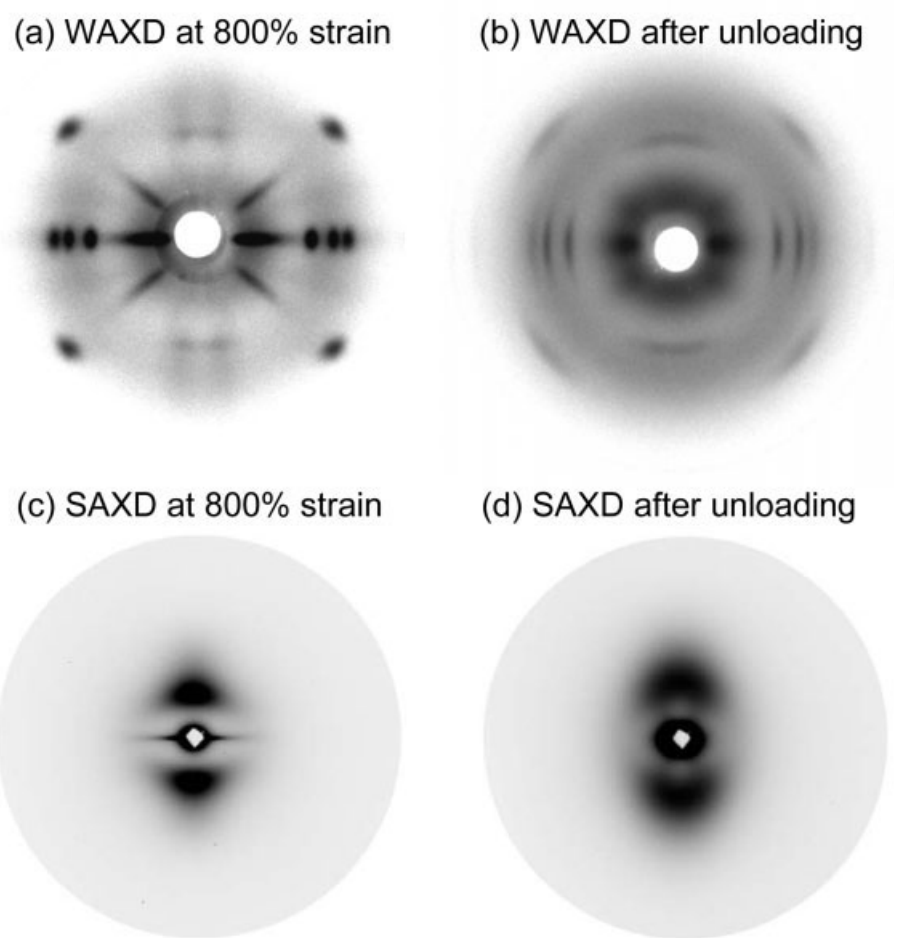

Figure 7 Effect of unloading on the WAXD and SAXD patterns of P/E: (a) WAXD at the conditioning strain of 800%; (b) WAXD after unloading; (c) SAXD at the conditioning strain of 800%; and (d) SAXD after unloading.

crosslinked chains assuming a functionality of four, α is the chain inextensibility, and ϕ is defined as

$$\varphi = \lambda^2 + \frac{2}{\lambda} \tag{2}$$

Equation (1) did not describe the conditioning curve very well or the first cycle curve if the conditioning strain was less than 400%. However, if the conditioning strain was 400% or more, the fit was very good (Fig. 10). The values of N_c and α that gave the best fit

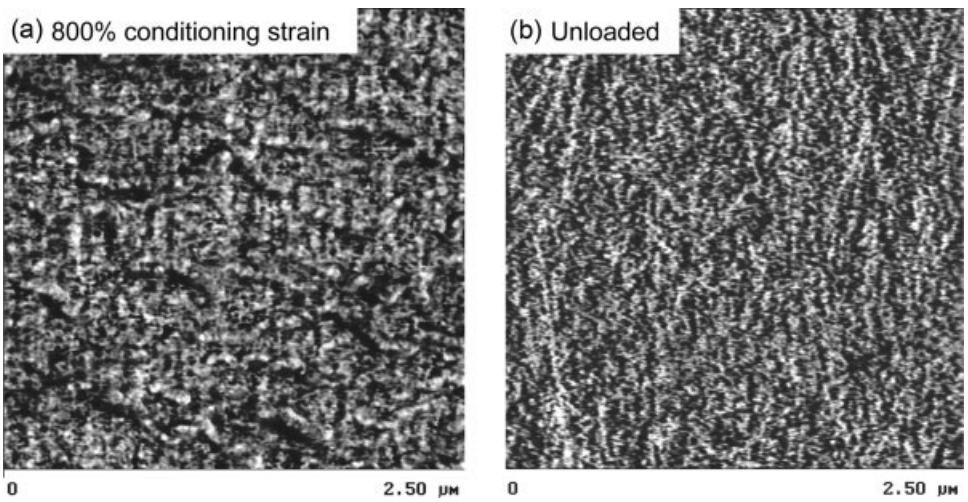

Figure 8 AFM phase images of P/E: (a) at the conditioning strain of 800%; and (b) after unloading.

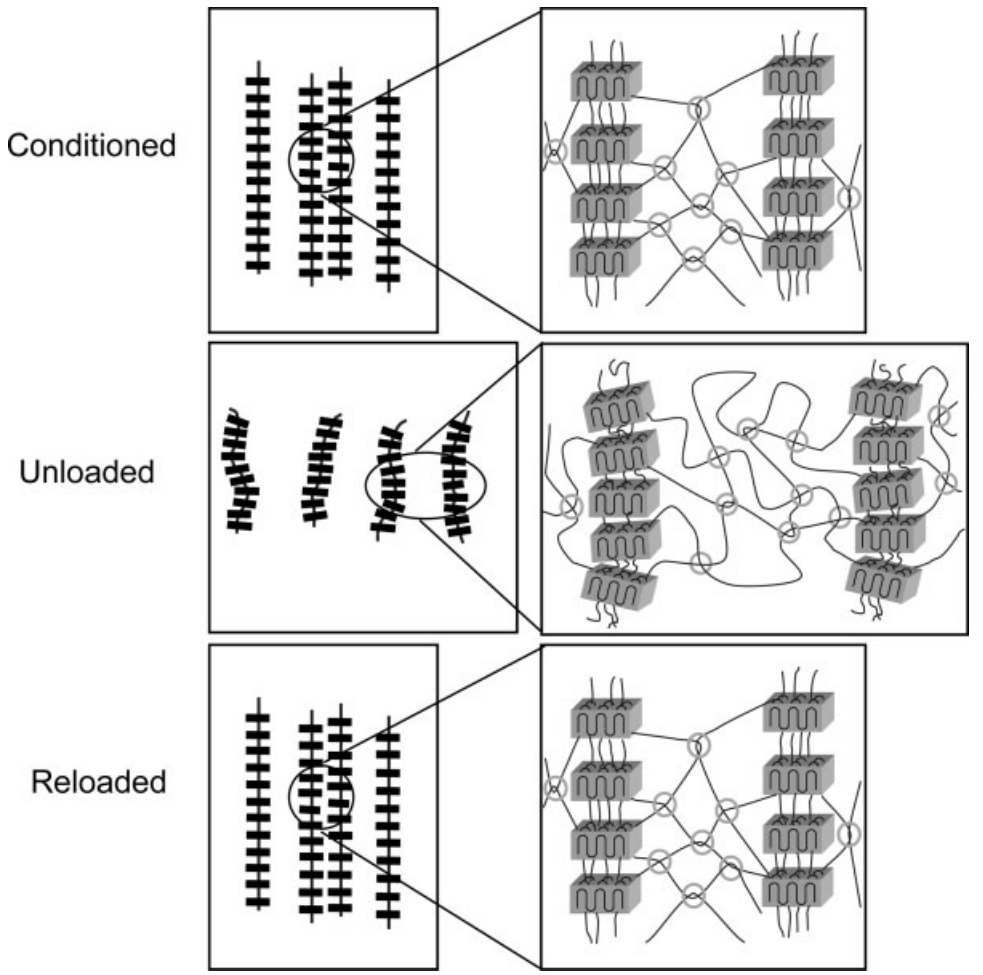

Figure 9 The proposed structural model for elastomeric behavior of conditioned P/E.

are given in Table I. Between 400 and 800% conditioning strain, N_c increased only slightly, which reflected relatively small differences in the initial part of the stress–strain curve. However, doubling of α between 400 and 800% conditioning strain reflected the very large increase in strain hardening.

The molecular weight of the chain segment between crosslinks M_c was obtained from N_c according to

$$M_c = \frac{\rho N_A}{N_c} \tag{3}$$

where ρ is the density and N_A is Avogadro's number. The extracted M_c values in Table I were almost independent of the conditioning strain; moreover, the magnitude of M_c was intermediate between the entanglement molecular weights of 5000 g mol^{-1} for polypropylene and 1000 g mol^{-1} for polyethylene.[23] This supported the proposed structural model in which entanglements of the amorphous chains acted as network junctions and provided the elastic response. The shish-kebab fibers were seen as constraining extension of the amorphous chains, and thereby providing the strong strain hardening behavior of conditioned P/E.

Creation of a low crystallinity, elastomeric material by conditioning may not be unique to P/E copolymers. To test the generality of the phenomenon, an EO copolymer with approximately the same low level of crystal-

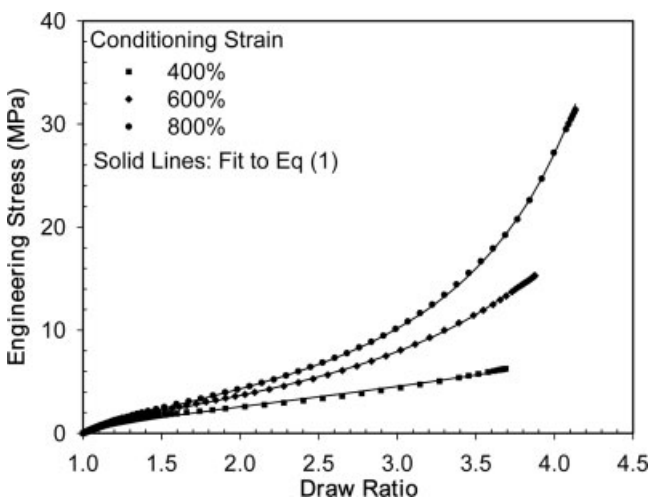

Figure 10 Fit of eq. (1) with the first cycle loading curve of P/E for various conditioning strains.

TABLE I
Crosslink Model Parameters

Conditioning strain (%)	α	N_ckT (MPa)	N_c (10^{-25} m^{-3})	M_c (g mol^{-1})
400	0.085	1.38	34	1,500
600	0.154	1.70	42	1,200
800	0.172	1.89	47	1,100

linity as P/E was conditioned in the same way. In contrast to the lamellar crystals that persist in P/E copolymers even at low levels of crystallinity, EO copolymers of low crystallinity possess fringed micellar crystals.[2]

The initial conditioning cycles of P/E and EO to 800% strain are compared in Figure 11(a). Both had approximately the same initial modulus because of similar crystallinities. However, at higher strains, P/E exhibited much stronger strain-hardening. Multiple conditioning cycles were required before EO exhibited constant loading and unloading cycles, and complete recovery. After conditioning, EO showed a much weaker stress response than P/E [Fig. 11(b)].

The lower stress response of conditioned EO may result from the granular, fringed micellar crystal struc-

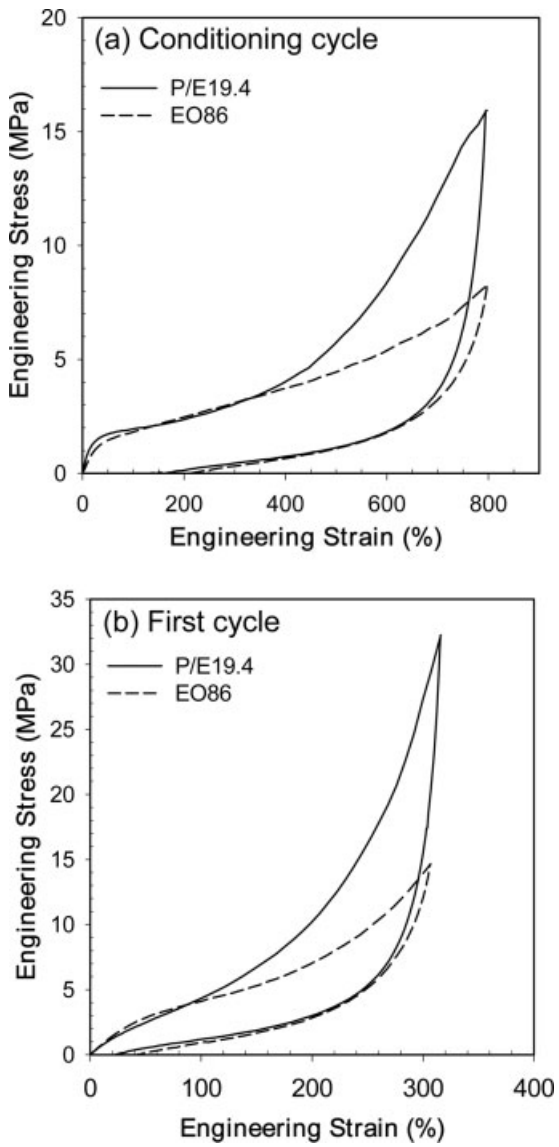

Figure 11 Comparison of P/E and EO: (a) Conditioning cycle to 800% strain; and (b) first cycle.

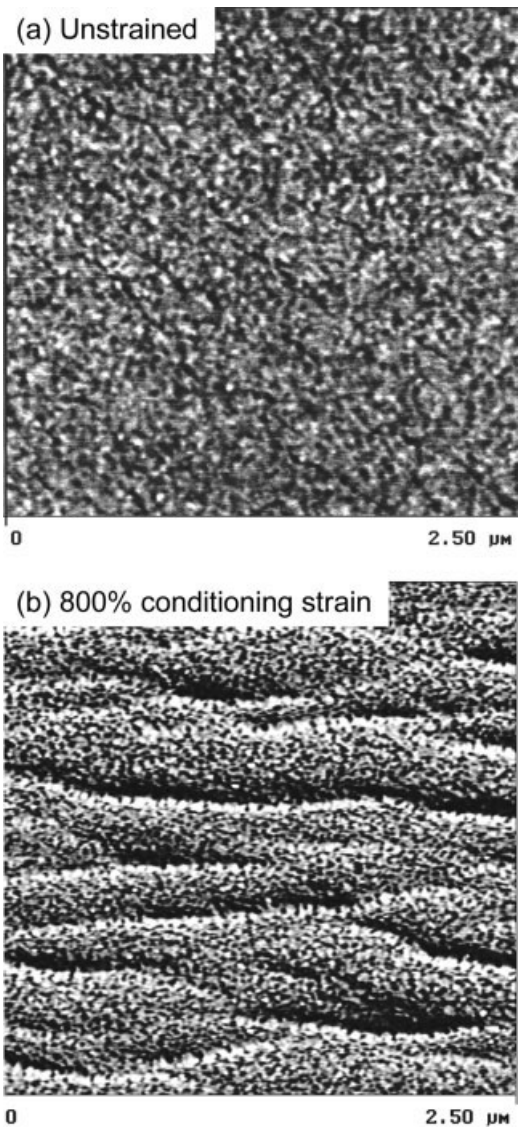

Figure 12 AFM phase images of EO: (a) unstrained; and (b) at 800% strain. The stretching direction is vertical. The wavy, horizontal features are an artifact.

ture that imparts elastomeric behavior to EO [Fig. 12(a)]. Because octene comonomer is excluded from the polyethylene crystal, methylene sequences that are not long enough to chain fold crystallize as fringed micellar crystals. Under stress, micellar crystals are imagined to ''melt'' and ''recrystallize'' by detachment and reattachment of crystallizable chain segments,[4] processes whereby the fringed micellar crystal structure is preserved. Even when stretched to 800% strain, EO retains the granular morphology of fringed micellar crystals [Fig. 12(b)]. It is significant that the WAXD pattern of stretched EO shows no evidence of a crystalline fiber pattern. Rather, the diffuse halo that is characteristic of the small micellar crystals persists in conditioned EO.

CONCLUSIONS

This work extended the possibilities for polyolefin-based thermoplastic elastomers, previously demonstrated with EO copolymers, to P/E copolymers. An initial ''conditioning'' extension to 800% strain resulted in a P/E elastomer with low initial modulus, strong strain hardening at high strain, and complete recovery over many cycles. Characterization of the structural changes at various strains during the conditioning process revealed the transformation of crystalline lamellae into shish-kebab fibers by melting and recrystallization.

The shish-kebab fibers, accounting for only 5% of the bulk, were interconnected by a matrix of entangled, amorphous chains that constituted the remaining 95%. It was proposed that the fibers acted as a scaffold to anchor the amorphous rubbery network. Entanglements of the amorphous chain segments functioned as network junctions and provided the elastic response. The stress–strain response of materials conditioned to 400% strain or more was described by the classical rubber theory with strain hardening. The extracted value of M_c, the molecular weight between network junctions, was intermediate between the entanglement molecular weights of polypropylene and polyethylene in accordance with the structural model of deformation. The strong stress response at high strains, as reflected in the inextensibility parameter α, was attributed to constraints imposed by shish-kebab fibers on the amorphous network.

The shish-kebab morphology was not obtained in a similarly conditioned EO elastomer. This was attributed to differences in crystalline morphology. In contrast to lamellar crystals that persisted in low crystallinity P/E, EO with low crystallinity possessed fringed micellar crystals. Apparently, fringed micellar crystals functioned as mobile network junctions that accommodated high strains by detachment and reattachment of crystallizable chain segments. The fringed micellar crystals of EO did not transform into shish-kebab fibers. As a consequence, the elastomeric EO did not exhibit the strong stress response at high strains that was characteristic of elastomeric P/E.

The authors thank Dr. Brian Landes and Dr. Lizhi Liu of The Dow Chemical Company for their assistance with the SAXS measurements. The authors are also pleased to acknowledge the helpful discussions with Dr. Andy Chang of The Dow Chemical Company. The research was generously supported by The Dow Chemical Company.

References

1. Meckel, W.; Goyert, W.; Wieder, W. In Thermoplastic Elastomers: A Comprehensive Review; Legge, N. R., Holden, G., Schroeder, H. E., Eds.; Hanser: Munich, 1987; Chapter 2.
2. Bensason, S.; Minick, J.; Moet, A.; Chum, S.; Hiltner, A.; Baer, E. J Polym Sci, Part B: Polym Phys 1996, 34, 1301.
3. Minick, J.; Moet, A.; Hiltner, A.; Baer, E.; Chum, S. P. J Appl Polym Sci 1995, 58, 1371.
4. Bensason, S.; Stepanov, E. V.; Chum, S.; Hiltner, A.; Baer, E. Macromolecules 1997, 30, 2436.
5. Hiltner, A.; Dias, P. S.; Poon, B.; Ronesi, V.; Chang, A.; Ansems, P.; Baer, E. ANTEC 2003 SPE Conference Proceedings 2003, pp 1780–1784, .
6. Dias, P.; Hiltner, A.; Baer, E.; Ansems, P.; Chum, S. ANTEC 2004 SPE Conference Proceedings 2004, pp 2596–2599.
7. Dias, P.; Wang, H.; Nowacki, R.; Chang, A.; Van Dun, J.; Ansems, P.; Chum, S.; Hiltner, A.; Baer, E. ANTEC 2005 SPE Conference Proceedings 2005, pp 1227–1231.
8. Toki, S.; Sics, I.; Burger, C.; Fang, D.; Liu, L.; Hsiao, B. S.; Datta, S.; Tsou, A. H. Macromolecules 2006, 39, 3588.
9. Wunderlich, B. Macromolecular Physics, Vol. 3; Academic Press: New York, 1980; p 63.
10. Olley, R. H.; Bassett, D. C. Polymer 1982, 23, 1707.
11. Zimmermann, H. J. J Macromol Sci Phys 1993, 32, 141.
12. Andersen, P. G.; Carr, S. H. J Mater Sci 1975, 10, 870.
13. Norton, D. R.; Keller, A. Polymer 1985, 26, 704.
14. Samuels, R. J. J Polym Sci, Part A: Gen Pap 1965, 3, 1741.
15. Chang, A. D.; Tau, L.; Hiltner, A.; Baer, E. Polymer 2002, 43, 4923.
16. Spruiell, J. E.; White, J. L. Appl Polym Symp 1975, 27, 121.
17. Ran, S.; Zong, X.; Fang, D.; Hsiao, B. S.; Chu, B.; Phillips, R. A. Macromolecules 2001, 34, 2569.
18. Balta-Calleja, F. J.; Peterlin, A. J Mater Sci 1969, 4, 722.
19. Sauer, B. B.; McLean, R. S.; Brill, D. J.; Londono, D. J. J Polym Sci, Part B: Polym Phys 2002, 40, 1727.
20. Ward, I. M.Ed. Structure and Properties of Oriented Polymers; Chapman & Hall: London, 1997; p 142.
21. Treloar, L. R. G. The Physics of Rubber Elasticity; Oxford University Press: London, 1967.
22. Edwards, S. F.; Vilgis, Th. Polymer 1986, 27, 483.
23. Fetters, L. J.; Lohse, D. J.; Ricter, D.; Zirkel, T. A. Macromolecules 1994, 27, 4639.